

Identification of a Driver Steering Model, and Model Uncertainty, From Driving Simulator Data

Liang-Kuang Chen

A. Galip Ulsoy

Department of Mechanical Engineering,
University of Michigan,
Ann Arbor, MI 48105-2125

For active safety systems that function while the driver is still in the control loop, driver uncertainty can affect system performance significantly. In this paper, an approach to obtain both the driver model and its uncertainty from driving simulator data is presented. The structured uncertainty is used to represent the driver's time-varying behavior, and the unstructured uncertainty for unmodeled dynamics. The uncertainty models can represent both the uncertainty within one driver and the uncertainty across multiple drivers. The structured uncertainty suggests that an estimation and adaptation scheme might be applicable for the design of controllers for active safety systems.

[DOI: 10.1115/1.1409554]

1 Introduction

Vehicle active safety systems are designed to improve driving safety while the driver is still in control of the vehicle. For the design of such systems, driver-controller interaction can be significant and should not be neglected. Pilutti [1] shows that a lane departure warning system can be improved by considering variations in driver state. An active controller that uses direct intervention of vehicle motion will lend to driver-controller interaction issued, and generally requires a thorough investigation of driver behavior before active safety controllers can be implemented [2–4].

For vehicle lateral control, the steering wheel angle is the primary means for control actuation. Many driver models try to approximate the real driver's road tracking performance, assuming certain driver inputs and outputs. Several driver models have been developed in the literature (e.g., [5–9]). A well-known result from human factors research is the “crossover” model [5,6]. The crossover model states that the open loop frequency response of the driver-vehicle combination approximates that of transfer function ω_c/s around the crossover frequency, where ω_c is the crossover frequency. Many driver models can be regarded as different realizations of the crossover model (e.g., [7,8]). These models have similar characteristics around the crossover frequency and differ more at higher and lower frequency ranges. Models of the driver steering control, based on system identification, which can be used for on-line implementation have also been reported in [10,11].

Although these models approximate the driver behavior well, no driver model is expected to represent the real driver completely. Furthermore, for the purpose of controller design, it is common practice to use a low-order driver model. Therefore, it is reasonable to expect that significant driver model uncertainty exists. This driver model uncertainty can have a significant effect on the performance of the designed control system. To successfully design an active safety controller, including warning and direct intervention, it is necessary to obtain a reasonable representation of this driver model uncertainty. The uncertainty can be used to represent the difference between one real driver and the driver model at any instant in time, or to represent the change in driving behavior with time. On a larger scale, the uncertainty can also be used to represent the variation across several different drivers if the designed system is to be used by different drivers. However, studies of driver model uncertainty have not been reported in the

literature. This article aims to develop a model for the driver model uncertainty using the measured data from real drivers driving a fixed-base driving simulator.

In general, model uncertainty can be divided into structured uncertainty (e.g., parametric uncertainty) and unstructured uncertainty (e.g., additive uncertainty due to unmodeled dynamics). Driver model uncertainty includes contributions from: model order, parameter uncertainty, and nonlinearity [12]. In this study, the parametric uncertainty is used to represent the variation of driver behavior during a period of time. The unstructured uncertainty is used to account for unmodeled dynamics and nonlinearity of the real driver. Intuitively, higher order models can capture additional dynamic characteristics of the real driver, and can be considered more “complete.” If a linear low order model is used for the driver, the difference in model order will contribute to the model uncertainty. From the controller design viewpoint, the parametric uncertainty may be dealt with using adaptive control techniques and the unstructured uncertainty may be addressed using robust control techniques. The contribution of this research work is a new approach to compute the driver model with parametric and unstructured uncertainty from driving simulator data.

2 Identification of Driver Model From Simulator Data

In this study it is proposed to use system identification techniques and driving simulator data to obtain a driver model and the model uncertainty. We consider a black-box driver model where the lateral deviation from the centerline of the road (y) is treated as the input of the driver. The driver's output is the steering wheel angle (δ). The idea of this model is shown schematically in Fig. 1. The objective of this research is to obtain a nominal driver model (G_d) with parametric uncertainty and unstructured model uncertainty (Δ) from the driving simulator data. This idea is shown in Fig. 2, where an additive model uncertainty is used. It is noted that the measured δ is not completely related to the input signal y . Therefore, a disturbance term e' is used to represent the portion of the data that cannot be included in Δ . In order to understand the identification results more clearly, it is helpful to examine the data in more detail.

2.1 The Data. The data used for system identification was collected from a series of driving simulator tests. The Ford Driving Simulator (FDS) was used to conduct these experiments. An example screen display picture is shown in Fig. 3. Twelve subject drivers, each driving for two hours, were requested to drive the simulator in a typical highway driving scenario. The experimental conditions have been designed to show the effect of fatigue on driving performance. The details of the experimental protocol and

Contributed by the Dynamics Systems and Control Division of THE AMERICAN SOCIETY OF MECHANICAL ENGINEERS. Manuscript received by the Dynamics Systems and Control Division January 17, 2001. Associate Editor: S. Passolis.

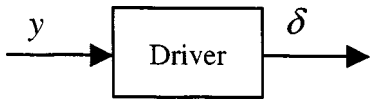


Fig. 1 Black-box driver model

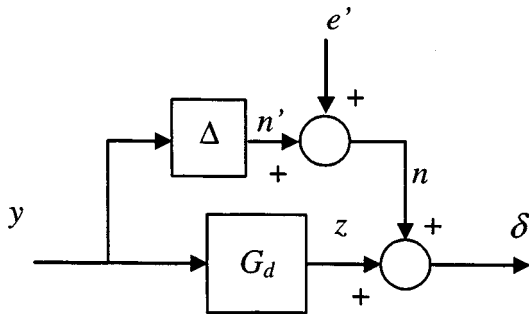


Fig. 2 Desired driver model



Fig. 3 Sample driving simulator scene

data acquisition can be found in [10]. A sample data plot of the input (y) and output (δ) signals is shown in Fig. 4. A block diagram to illustrate the experimental setup is shown in Fig. 5. In Fig. 5, the driver uses the steering command (δ) to control the driving simulator (FDS), and uses simulator output as his input. Therefore, the existence of the feedback path is clear.

It has been decided to use lateral position error (y) as the driver model input and driver's steering angle command (δ) as output. The lateral position error is defined as the distance from the vehicle center of gravity to the center of the lane. Examining the original data (e.g., Fig. 4) indicates that different drivers exhibit different mean lateral position error. This is an indicator of different drivers' driving performances, and is not the characteristic of driver behavior to be modeled. Therefore, the mean lateral position error was removed from each driver's data.

Furthermore, in order to represent change in driving behavior during the 2-hr test, the data was divided into 120 segments, with each segment being 1-min long. It is desired to have a smaller length for each segment of data so that the driver behavior is more "stationary" in each segment. However, it is shown in Fig. 6 that the driver steering command usually is slower than 0.5 Hz. The information in the data may be lost if not enough data points are used in each segment. Therefore, it is decided to use 1-min. for the length of each segment. A reverse arrangements test is applied on each segment of data to test the stationarity with each segment [13]. It is found that about 95% of the 120 segments can meet the

reverse arrangement requirement, indicating that the data within each segment can be regarded as stationary. The test for the overall 2-hr data indicates that the stationarity requirement is not satisfied in general. This supports the assumption that the driver behavior varies during the long driving task. The system identification is performed on each segment of data to obtain a set of driver model parameters for the 1-min interval. This is used to illustrate how the driver model parameters vary with time during the 2-hr driving period.

A sample signal spectrum is shown in Fig. 6. It is observed that both the input and output signals consist of very low frequency, mostly under 1 Hz, as can be seen in Fig. 6. Therefore, although the original data is samples at 20 Hz, the data used for system identification is resampled at 10 Hz. There is no prefiltering to

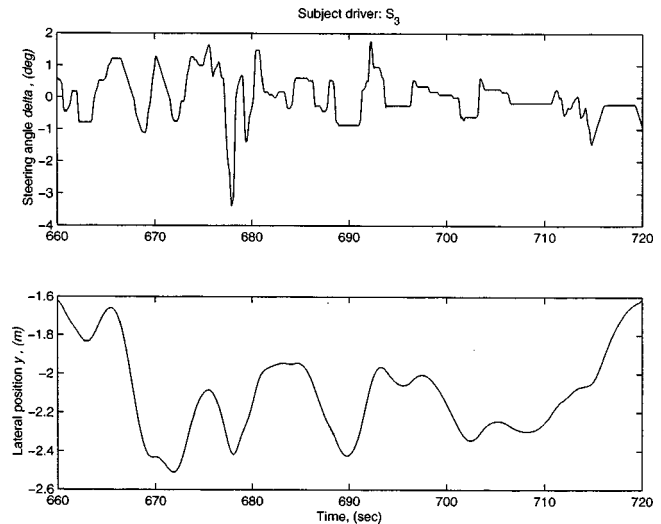


Fig. 4 Sample driving simulator data

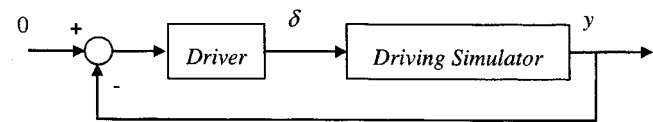


Fig. 5 Schematic of the experimental setup

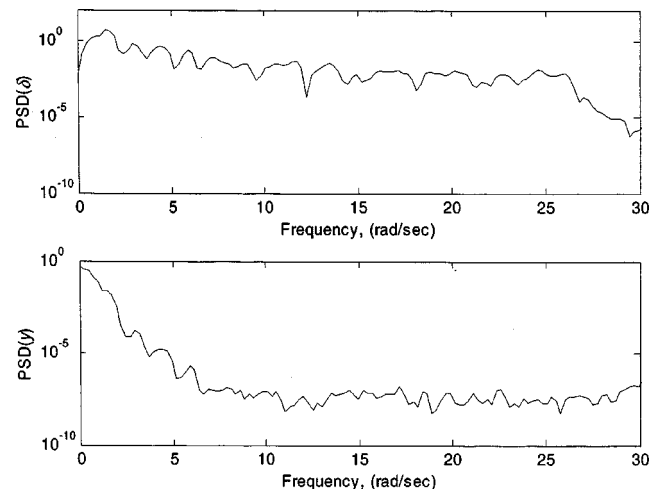


Fig. 6 Sample signals spectrum

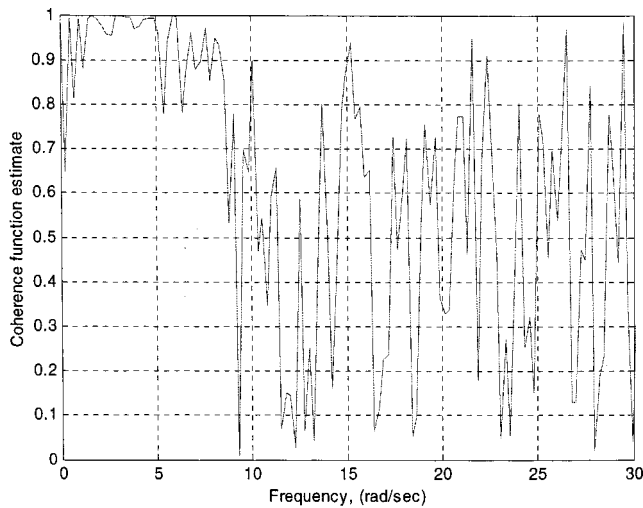


Fig. 7 Sample coherence spectrum

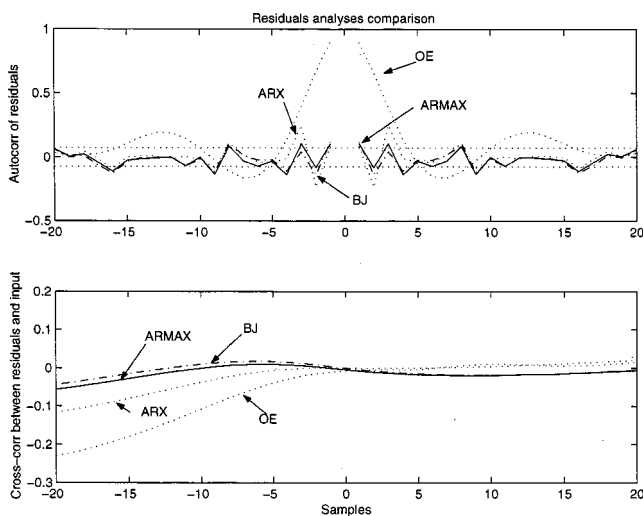


Fig. 8 Comparison of different model residuals

prevent aliasing, because at frequencies near the Nyquist frequency, both input and output signals are almost 200 dB less than the magnitude in the low frequency range.

A sample of the coherence spectrum is also shown in Fig. 7. It is found that the input-output data has a reasonably good linear relation up to 1 Hz. Above 1 Hz, the frequency content is low and the coherence degrades rapidly. Therefore, it should be noted that the resulting models are not accurate above 1 Hz since the linear relation between input and output is not good in those frequency ranges.

2.2 Driver Model Structure. The selection of model structure is a compromise between model accuracy and simplicity. It has been decided to use a parametric model structure for its simplicity in identification computations and the utility of the resulting models for controller design purpose. The auto-regression with exogenous inputs (ARX) model structure is one of the simplest parametric structures one can use and is chosen as the first structure to begin with. However, the residual analysis indicates that, in general, the auto-regression moving average with exogenous inputs (ARMAX) structure can yield residuals closer to white noise, given the same model order. An example of this comparison is shown in Fig. 8, where the 99% confidence intervals are also shown in the auto-correlation plot. This implies that the ARMAX model structure is a better choice than the ARX

structure. Other model structures are also available, for example, the Box-Jenkins (BJ) and output error (OE) models [14]. Figure 8 indicates that the ARMAX and BJ structures can yield the best residual whiteness. Therefore, the ARMAX structure is chosen here to model the driver because it has fewer parameters to be estimated than the BJ structure. The ARMAX driver model can be written as:

$$A \delta(t) = B y(t) + C e(t) \quad (1)$$

where A , B , and C are time-invariant polynomials in the time shift operator q to be identified for each segment of data. The ARMAX model can be represented in the block diagram shown in Fig. 9, where e is the white noise that goes into the driver model and δ is the predicted driver's output. Polynomials A and B are used to represent the nominal driver model. That is, in Fig. 2, $G_d = B/A$ and z in Fig. 2 is equal to \hat{z} in Fig. 9.

Once the ARMAX structure is chosen, it is necessary to determine the order of each polynomial and the delay term in the model. The general approach used is to try many combinations of order and delay, and the set that can give "best" prediction error with the desired model order is chosen. The trade-off between model order and prediction error has been widely studied, e.g., the Akaike information criteria (AIC) [15] and final prediction error (FPE) criteria [16]. Due to the large number of data (600 data points in each segment), the above two criteria generally suggest high order models. For example, the FPE can be written as [14]:

$$\bar{J}_p \approx \frac{1 + (d_M/M)}{1 - (d_M/N)} V_N \quad (2)$$

where N is the number of data points and d_M is the number of parameters in the model. V_N is the mean square value of model prediction error. It is seen that the first term in Eq. (2) penalizes on increasing model order. For $N=600$, this penalty will not be significant until large value for d_M (e.g., about 7% increase for $d_M = 20$). However, such high order models are undesirable. Furthermore, the residual analysis results indicate that increasing the model order does not improve residuals whiteness significantly. The purpose of this work is to find a low order driver model that is easier to use in controller design. Consequently, it is decided to keep two parameters in polynomials A and B , and use one sampling interval of delay and one term in C . That is, the ARMAX model can be represented by (as described in Eq. (1))

$$\begin{aligned} A &= 1 + a_1 q^{-1} + a_2 q^{-2} \\ B &= (b_1 + b_2 q^{-1}) q^{-1} \\ C &= 1 + c_1 q^{-1} \end{aligned} \quad (3)$$

The identified driver model is a phase lead filter with delay. This structure agrees with most existing driver models in the literature. Furthermore, the resulting nominal driver model agrees with the crossover principle, as shown in Fig. 10.

2.3 Identification in Closed-Loop. It can be seen from Fig. 5 that the experiments were conducted in a closed-loop configuration. The existence of feedback can also be seen from the

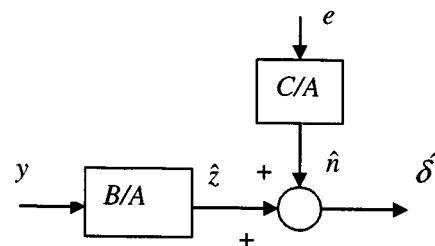


Fig. 9 Block diagram of ARMAX driver model

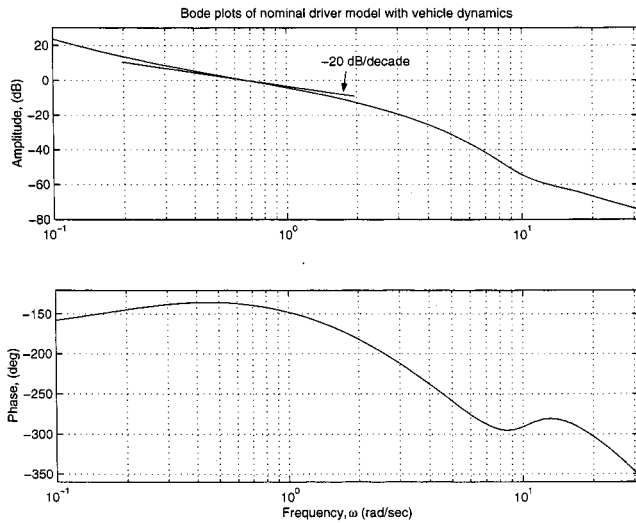


Fig. 10 Bode plots of nominal driver model/vehicle system

residual analysis plots. That is, in Fig. 8, the cross-correlation between the residual and the input becomes large for a negative lag.

The system identification approach demands “richness in excitation,” especially in closed-loop. Thus the experiments were designed to include ground unevenness as a disturbance to the simulation [10]. The bicycle model of vehicle lateral dynamics contains two poles at the origin and two poles at around 1 Hz. However, the lateral dynamics in the FDS is much more complex than this bicycle model. It is assumed that the lateral dynamics is complex enough, and it does not filter out useful information in the data over the frequency range of interest. The persistent excitation requirement of the lateral position error (y) can be tested based on the covariance matrix [14]. If the input signal covariance matrix ($R_u(N)$) is positive definite for a positive integer N , the signal is said to be persistently exciting of order N . The input signal is tested based on this criteria for $N=4$, and is found to satisfy this requirement for the data tested. Since the model has been selected to be low order, a persistently exciting input of order 4 is sufficient. It is well known that the models obtained using spectral and correlation methods are not reliable for data collected from closed-loop experiments [14]. Therefore, the prediction error method for system identification is employed. This method is applied in a straightforward manner, that is, as if there were no feedback. This is termed “The Direct Approach” in [14], where it is also note that the estimated models can be biased if the noise model is not sufficiently accurate. In Section 2.2, several different combinations of model orders have been investigated and they are shown to yield similar whiteness in the residuals. The consistency in the residual analysis justifies the noise model used.

3 Uncertainty Modeling

Modeling uncertainty from experimental data is a challenging task. There is no standard approach for computing such models. The main purpose of this section is to illustrate how the uncertainty models are obtained after the driver model is identified. Both structured and unstructured uncertainties of the driver model are considered here. The driver model used in this work does include a delay element, however, the variation of the delay is not considered. Any other nonlinearity inherent in the driver steering behavior will contribute to the unstructured uncertainty.

It is proposed that the $|\Delta|$ in Fig. 2 be defined as the magnitude of the transfer function relating y and n' . However, n' cannot be computed directly from the data. If the driver model (G_d) in Fig. 2 is replaced by the identified ARMAX model of driver (B/A) in

Fig. 9), the signal z in Fig. 2 can be computed from the driver model and measurement data. Consequently, n can be computed as $n = \delta - z$, where $z = (B/A)y$ from the ARMAX model in Fig. 9, and is used in the computation of $|\Delta|$. A spectral analysis with n and y can give an estimated transfer function of $|\Delta|$. That is,

$$|\Delta| = \left| \frac{\frac{1}{\sqrt{N}} \sum_{t=1}^N n(t) e^{-i\omega t}}{\frac{1}{\sqrt{N}} \sum_{t=1}^N y(t) e^{-i\omega t}} \right| \quad (4)$$

where N is a positive integer indicating the number of data points. However, as discussed in Section 2.3, the closed-loop experiments may cause the identified models based on spectral methods to be unreliable. Therefore, a parametric model approach is employed. With y as input, and $n = \delta - z$ as output, a second order ARX model for $|\Delta|$ is obtained. The coherence between y and n is close to unity for frequencies up to 1 Hz, justifying the linear ARX structure. Thus $|\Delta|$ can be computed for each data segment from y and n . The upper bound of $|\Delta|$ within the 2-hr driving task for one driver, or across several different drivers can then be obtained.

In order to describe the time varying behavior of the driver, the two-hour data set is divided into 120 one-minute segments. The first segment of data is ignored because at the beginning of the experiments, some signals were not measured. As a result, 119 segments of data are available for each driver. For each segment of data, the ARMAX driver model parameters are estimated. These 119 sets of data will be used to identify and validate the driver model. The mean value, standard deviation, minimum, and maximum for the parameters of driver model can be calculated. The variation of model parameters represents the driver’s time-varying behavior during the two-hour driving test.

4 Identification Results Model Validation and Discussion

The driver model uncertainty developed here is intended for controller design. Two different application scenarios are considered. The first scenario is to use the uncertainty model developed to design a steering assist system to be used for a specific driver. The advantage of this application is less uncertainty will be obtained, and this is a benefit for controller design. The cost for this advantage is that a “learning” system to estimate the particular driving preference of a driver is needed. Another scenario is to generalize the driver model uncertainty to include the variation across different drivers, in addition to the variation within one driver. The driver model uncertainty developed for this purpose will be larger than the previous case, thus increasing the difficulty in the controller design phase. Based on the method described in the previous section, both situations are considered and summarized in the following two sections.

4.1 Uncertainty With One Driver. System identification is used to estimate the ARMAX model using data from one driver. The 120 segments of data are divided into two groups. The odd numbered segments of the data are used for identification purposes. The even numbered segments of data will be used for validation. That is, the model uncertainty results for the validation sets are compared to the results of the estimation data. There are cases where the identification algorithm yields poles that are unstable or negative in the discrete domain. These results are unreasonable and are considered as outlier points. This may result from the fact that the particular segments of data are not suitable to be modeled by an ARMAX model. Therefore, those segments are removed from the data set. Figure 11 shows the parameter variation of the driver model. The mean and standard deviation of the parameters are summarized in Table 1. Their significance can be presented by the corresponding pole-zero locations, and DC gain., as shown in Fig. 12. Figure 12 shows the equivalent pole-zero

locations in the continuous time domain. The pole-zero mapping technique has been applied for conversion from discrete time to continuous time. That is, the $z = e^{Ts}$ transformation is used, where the sampling time T is 0.1 sec in this study. The results show that in general one of the system poles is close to the origin, indicating it is the dominant pole. The location of the second pole is rather unpredictable. In contrast, the location of the only zero of the model is usually between 0 and -1 , and very close to the origin in

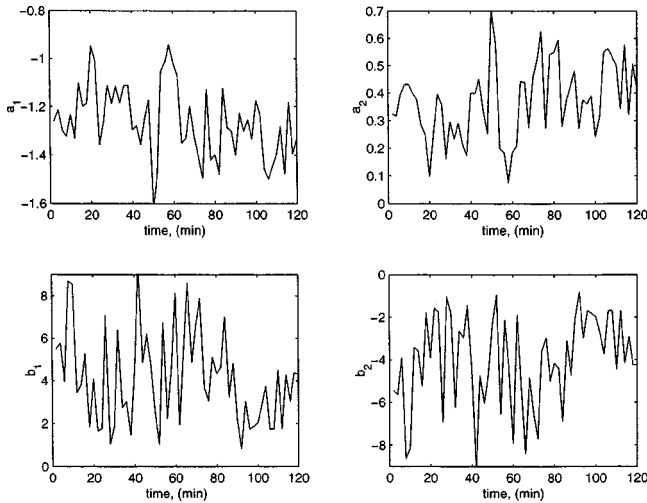


Fig. 11 Driver model parameter variations

Table 1 Driver model parameters: one driver

One driver		a_1	a_2	b_1	b_2
estimation	mean	-1.2623	0.3697	4.1340	-4.0337
	std	0.1485	0.1379	2.2013	2.1557
validation	mean	-1.2537	0.3564	4.2202	-4.1244
	std	0.1264	0.1295	2.1071	2.0766

most cases. This is expected since the driver model includes a phase lead. The DC gain can vary widely between 0.2 and 2.

The parametric uncertainty indicates that the driver steering behavior changes significantly with time. The large variation in DC gain indicates that the driver generates different steering commands in response to same lateral position error at different times. The variation of pole-zero locations implies that the response speed of the driver also changes with time. Therefore, this uncertainty can be useful when a controller is needed to suppress the effect of driver performance degradation in time. If an on-line estimation of parameters algorithm is implemented, it could be possible to design an adaptive control law to achieve this goal. Robust control techniques, e.g., QFT and H_∞ , can also be used to handle the parametric uncertainty [17].

The estimate of the unstructured uncertainty has been described in Section 3. The resulting uncertainty $|\Delta|$, obtained from the odd numbered segments of data, is shown in Fig. 13. A first-order transfer function is tuned to roughly envelop the uncertainty curves. The resulting upper bound is shown in Fig. 14, and can be represented as

$$|\Delta_i(\omega)| = \left| \frac{0.5 + 5j\omega}{2.5 + j\omega} \right| \quad (5)$$

A dashed line is included in Fig. 13 showing the frequency of 1 Hz. As shown in Fig. 6, generally the data has very small magnitudes above this frequency. Therefore, the identification results above 1 Hz are unreliable and should be discarded. The sources of unstructured uncertainty include the random behavior of the driver and any unmodeled dynamics (model order, nonlinearity, etc). In [18], the authors investigated the ‘‘complacency’’ nonlinearity that is evident from the data. It is concluded that although including the complacency nonlinearity can improve the model prediction, the resulting unstructured uncertainty is not significantly reduced. The low order used in the driver model may also contribute to the unstructured uncertainty. Therefore, a fourth order driver model (G_d) is evaluated for comparison of the uncertainty due to model order. Figure 14 also shows the resulting unstructured uncertainty upper bound computed based on the fourth order G_d . It is seen

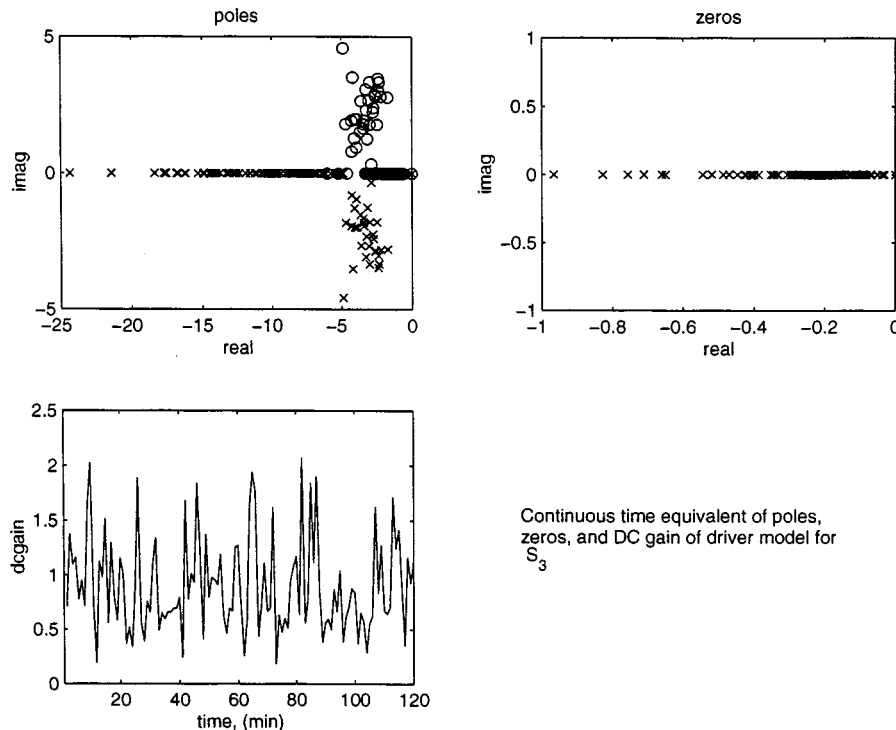


Fig. 12 Pole/zero and DC gain of driver model

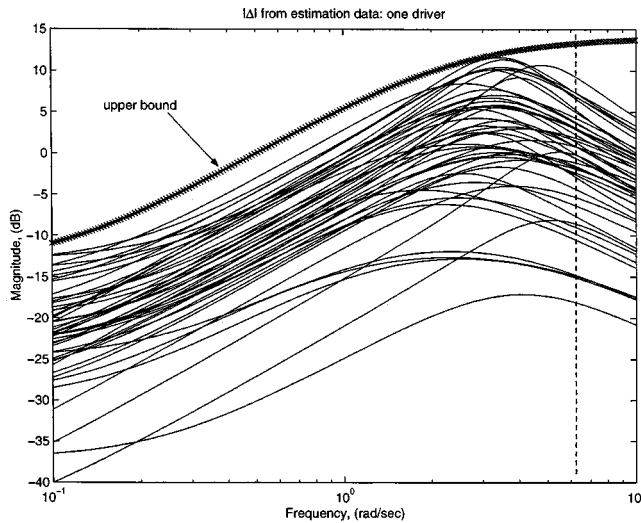


Fig. 13 Unstructured uncertainty: one driver

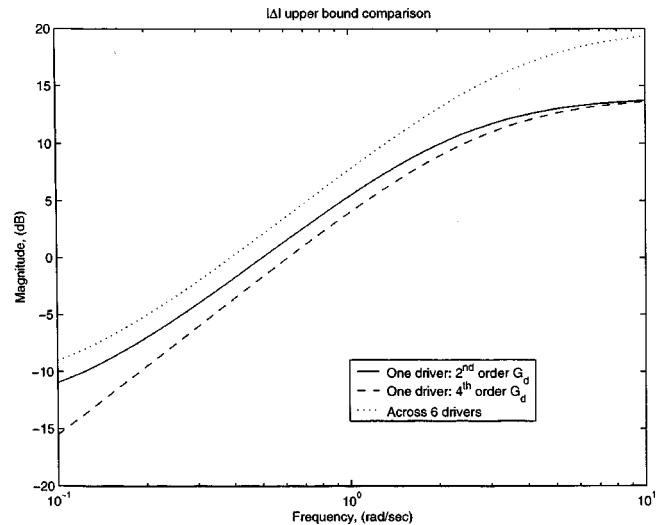


Fig. 14 Comparison of upper bounds on unstructured uncertainty

that the reduction in uncertainty is also very limited. It is believed that the unpredictability in driver behavior contributes most of the unstructured uncertainty.

4.2 Uncertainty Across Different Drivers. The same analysis is applied to the data from six different drivers, and a more general driver model uncertainty is obtained. The data from the other six drivers are reserved for validation purpose. The resulting unstructured uncertainty bound (for 6 drivers) is found to be larger than the bound for one driver, as shown in Fig. 14. The parameters' statistics for 12 drivers are listed in Table 2. Comparing Table 2 with Table 1, the change in the mean values of the parameters is expected. However, the decrease in the standard deviation is surprising. This is due to the fact that the particular driver (S_3) used in Section 4.1 is one of the drivers that has larger variation, as discussed in [10]. Therefore, after other lower uncertainty drivers' data is included, the standard deviation actually reduces. Nonetheless, the uncertainty across different drivers does cover similar range of values. If a system is designed to be used by many drivers, this result can be used to represent the variation across different drivers. However, it should be noted that some drivers may exhibit larger uncertainty, as outliers always exist.

4.3 Model Validation. The ARMAX model is validated by the fact that the residual is very close to white noise. An example has been shown in Fig. 8. The upper plot is the auto-correlation of the residuals and the lower plots is the cross-correlation between the residuals and the input to the driver, i.e., the lateral deviation. The auto-correlation plot lies within 99% confidence intervals for the ARMAX structure used. This shows that the residuals are very close to white noise, and therefore, the assumption for the ARMAX model holds. Figure 10 further justifies the identified driver model since the well-accepted crossover principle is satisfied.

To validate the uncertainty models, the data is divided into two groups. One group is used for estimation and the other group is used for validation. The resulting parameter distributions are listed in Tables 1 and 2. It is seen that although the means and standard deviations differ slightly between estimation and validation data sets, they compare relatively well. The unstructured uncertainty bounds shown in Fig. 14 are computed from the estimation data set. The unstructured uncertainties computed from validation data are tested against these upper bounds. The results show that the unstructured uncertainties from validation data lie below the upper bounds mostly, thus validating the upper bounds obtained from estimated data.

Table 2 Driver model parameters: twelve drivers

		a_1	a_2	b_1	b_2
estimation	mean	-1.3149	0.3979	3.7540	-3.6736
	std	0.1232	0.1233	1.7326	1.7031
validation	mean	-1.3162	0.4014	3.7334	-3.6520
	std	0.1222	0.1155	1.8401	1.8056

5 Summary and Conclusions

Vehicle active safety systems are designed to assist the driver while the driver is still in control of the vehicle. The design of such systems must consider the interaction from the driver. This article, for the first time, addresses the problem of modeling driver uncertainty from driving simulator data. The system identification approach to compute driver models is investigated and an algorithm to compute structured and unstructured uncertainty is presented. The resulting driver models have been verified using residual analyses and comparison to crossover models in the literature. The structured uncertainty is used to represent the driver's time-varying behavior. The unstructured uncertainty is used to represent the uncertainty due to unmodeled dynamics. The model uncertainty can be used to represent the uncertainty within one driver during driving, or it can be used to represent the uncertainty across different drivers.

The driver model obtained from system identification is shown to be appropriate in representing driver steering behavior. The structured uncertainty shows that the driver steering behavior changes with time significantly. It is observed that the unstructured uncertainty is significant, and the magnitude increases when going from uncertainty within one driver to uncertainty across several drivers. It has been shown that the model order and non-linearity (e.g., the "complacency" nonlinearity) do not contribute too much to the unstructured uncertainty. The variability in driver's steering behavior may be the primary source of the large uncertainty.

Future research to focus on the application of such uncertainty models is needed. Further research is also needed to validate the accuracy of the $|\Delta|$ presented here. The significant structured uncertainty suggests that an on-line estimation scheme with adaptive/robust control might be applicable. The unstructured uncertainty implies that a performant robust controller might be difficult to achieve. However, the unstructured uncertainty can provide insights to the characteristics of the driver uncertainty and the tradeoff between the achievable performance and uncertainty.

Acknowledgments

The authors would like to acknowledge the financial support from the Intelligent Transportation System Center (ITS), Research Center of Excellence (RCE). They also wish to thank Dr. Tom Pilutti at Ford Research Laboratories for providing the driving simulator data.

References

- [1] Pilutti, T., and Ulsoy, A. G., 1998, "Decision Making for Road Departure Warning Systems," *Proceedings of the 1998 American Control Conference*, Vol. 3, p. 1838–1842.
- [2] LeBlanc, D. J., Johnson, G. E., Venhovens, P. J. Th., Gerber, G., DeSonia, R., Ervin, R. D., Lin, C. F., Ulsoy, A. G., and Pilutti, T. E., 1996, "CAPC: Road-Departure Prevention System," *IEEE Control Syst. Mag.* **16**, No. 6 Dec, pp. 61–71.
- [3] LeBlanc, D. J., Venhovens, P. J. Th., Lin, C.-F., Pilutti, T. E., Ervin, R. D., Ulsoy, A. G., MacAdam, C., and Johnson, G. E., 1996, "Warning and Intervention System To Prevent Road-Departure Accidents," *Veh. Syst. Dyn.* **25**, No. Suppl, pp. 383–396.
- [4] Pilutti, T., 1997, "Lateral Vehicle Co-Pilot To Avoid Unintended Roadway Departure," Ph.D. thesis, University of Michigan, Ann Arbor, MI.
- [5] Weir, D. H., and McRuer, D. T., 1968, "Models for Steering Control of Motor Vehicles," *Proceedings, Fourth Annual NASA-University Conference on Manual Control* (NASA SP-192), p 135–169, U.S. Government Printing Office, Washington, DC.
- [6] Weir, D. H., and McRuer, D. T., 1973, "Measurement and Interpretation of Driver Steering Behavior and Performance," SAE Preprint n. 730098 for Meet Jan 8–12.
- [7] MacAdam, C., 1980, "An Optimal Preview Control for Linear Systems," *ASME J. Dyn. Syst. Mea., Control*, **192**, pp. 188–190.
- [8] Hess, R. A., and Modjtahedzaeh, A., 1990, "A Control Theoretic Model of Driver Steering Behavior," *IEEE Control Syst. Mag.* pp. 3–8.
- [9] Habib, M. S., 1994, "Characterization of Driver-Vehicle Directional Control Using Three Models of Human Driver," *Proc. Intl. Symp. On Advanced Vehicle Control [AVEC]*, Tsubaki, Japan.
- [10] Pilutti, T., and Ulsoy, A. G., 1999, "Identification of Driver State For Lane-Keeping Tasks," *IEEE Transactions on Systems, Man, and Cybernetics Part A: Systems and Humans*, **29**, No. 5, pp. 786–502.
- [11] Soma, H., and Hiramatsu, K., 1995, "Dynamic Identification of Driver-Vehicle System Using AR-method," *Veh. Sys. Dyn.* **24**, pp. 263–282.
- [12] MacFarlane, D. C., 1990, *Robust Controller Design Using Normalized Coprime Factor Plant Descriptions*, Springer-Verlag, Berlin; New York.
- [13] Bendat, J. S., and Piersol, A. G., 1986, *Random Data: Analysis and Measurement Procedures*, Wiley, New York.
- [14] Ljung, L., 1999, *System Identification: Theory for the User*, Prentice-Hall, Upper Saddle River, NJ.
- [15] Akaike, H., 1974, "A New Look At the Statistical Model Identification," *IEEE Trans. Autom. Control* **AC-19**, pp0. 716–732.
- [16] Akaike, H., 1969, "Fitting Autoregressive Models for Prediction," *Ann. Inst. Stat. Math.*, **21**, pp. 243–347.
- [17] Chen, L. K. and Ulsoy, A. G., 2000, "Robust Smith Predictor For Vehicle Steering Assist Control," *Proc. Intl. Symp. On Advanced Vehicle Control [AVEC]*, Ann Arbor, Michigan, pp. 67–73.
- [18] Chen, L. K. and Ulsoy, A. g., 2000, "Identification Of A Nonlinear Driver Model Via NARMAX Modeling," *Proceedings of the American Control Conference*, Vol. 4, pp. 2533–2537.